Geophysical Research Letters

RESEARCH LETTER
10.1029/2020GL088252

Precipitation-Induced Reduction in Surface Ocean pCO_2: Observations From the Eastern Tropical Pacific Ocean

David T. Ho[1] **and Julian J. Schanze**[2]

[1]Department of Oceanography, University of Hawai'i at Mānoa, Honolulu, HI, USA, [2]Earth and Space Research, Seattle, WA, USA

Key Points:
- Simultaneous measurements at the ocean surface and at 5 m show significant differences in pCO_2
- Rain affects surface ocean pCO_2 by mainly by dilution but also by temperature change
- Rain-induced changes in pCO_2 could significantly bias the determination of global air-sea CO_2 fluxes

Supporting Information:
- Supporting Information S1
- Data Set S1
- Data Set S2

Correspondence to:
D. T. Ho,
david.ho@hawaii.edu

Citation:
Ho, D. T., & Schanze, J. J. (2020). Precipitation-induced reduction in surface ocean pCO_2: Observations from the eastern tropical Pacific Ocean. *Geophysical Research Letters*, *47*, e2020GL088252. https://doi.org/10.1029/2020GL088252

Received 3 APR 2020
Accepted 17 JUL 2020
Accepted article online 29 JUL 2020

©2020. American Geophysical Union. All Rights Reserved.

Abstract Determining air-sea CO_2 fluxes using pCO_2 disequilibrium requires knowing the gas transfer velocity and air-sea pCO_2 difference. Most pCO_2 measurements are made from ships, whose uncontaminated seawater intakes are located at >5-m depth to prevent ingestion of air. However, there could be bias in determinations of CO_2 fluxes if there is disagreement between pCO_2 measurements at the surface and 5 m. Seawater measurements made at the near surface and 5 m in the eastern Equatorial Pacific Ocean show that precipitation can dilute surface seawater salinity and lower the pCO_2 and dissolved inorganic carbon and raise pH of the same water, and that these changes in ocean chemistry are largely missed by measurements at 5 m. This finding implies that estimates of ocean CO_2 uptake might be underestimated, since rain will lower surface ocean pCO_2 in both source and sink regions and, hence, increase uptake in sink regions and decrease outgassing in source regions.

1. Introduction

Changes in atmospheric CO_2 affect the radiative forcing of the planet and are responsible for the increase in global air and ocean temperatures and associated changes in the climate system and ecosystems on Earth. Between 2009 and 2018, anthropogenic activities such as fossil fuel burning, cement production, and land use and land use change released 40.2 Gt of CO_2 per year into the atmosphere, but 23% of this CO_2 emission was taken up by the ocean (Friedlingstein et al., 2019), thereby decreasing the atmospheric burden. The ocean is hence a significant sink for anthropogenic CO_2 emissions, and on short time scales, this flux of CO_2 between the atmosphere and the ocean (F_{CO_2}) is controlled by the gas transfer velocity (k_{CO_2}), and the difference in the partial pressure of CO_2 (pCO_2) in the water and the atmosphere (Δp_{CO_2}) is as follows:

$$F_{CO_2} = k_{CO_2} K_0 \Delta p_{CO_2}, \tag{1}$$

where K_0 is the solubility coefficient for CO_2, which varies as a function of water temperature and salinity (Weiss, 1974).

Gas transfer velocities over the coastal and open oceans are commonly parameterized as a function of wind speed using relationships derived from ^{14}C geochemical mass balances or $^3He/SF_6$ deliberate tracer release experiments (e.g., Ho et al., 2006; Nightingale et al., 2000; Wanninkhof et al., 2009). Surface ocean pCO_2 is often measured from research vessels or ships of opportunities, and maps of surface ocean pCO_2 have been made using different interpolation techniques (e.g., Landschützer et al., 2016; Rödenbeck et al., 2015; Takahashi et al., 2009). Atmospheric CO_2 is most often obtained from fixed stations (e.g., Mauna Loa or Cape Grimm) or from a global marine boundary layer CO_2 product (Dlugokencky et al., 2019; Masarie & Tans, 1995).

Rain has been shown to increase k_{CO_2} in both fresh and salt water (Ho, Bliven, et al., 1997; Ho et al., 2004; Takagaki & Komori, 2007; Zappa et al., 2009), which could increase F_{CO_2}. There are other factors that could affect F_{CO_2} by changing near-surface gradients of pCO_2 (see discussion in Woolf et al., 2019), including cool skin effects (e.g., Robertson & Watson, 1992; Van Scoy et al., 1995), microlayer salinity anomaly (e.g., Woolf et al., 2016), and diurnal warming and the resulting warm layer affect (e.g., McNeil & Merlivat, 1996). Furthermore, because rain contains negligible total alkalinity (TAlk) and only a small amount of dissolved inorganic carbon (DIC) compared to the surface ocean, rain can also dilute DIC and TAlk of the surface ocean, thereby lowering surface water pCO_2 (Turk et al., 2010). This effect would increase the ocean

uptake of atmospheric CO_2 because it would make Δp_{CO_2} (i.e., surface ocean pCO_2 minus atmospheric pCO_2) more negative in sink regions (i.e., where surface ocean pCO_2 is lower than the atmosphere) and make Δp_{CO_2} less positive in source regions (i.e., where surface ocean pCO_2 is higher than the atmosphere). However, until now, the phenomenon of rain lowering surface ocean pCO_2 through dilution has not been systematically documented in the open ocean, primarily because the intake ports of ships that make underway pCO_2 measurements are usually located far below the surface (at 5-m depth or greater).

Here, measurements of seawater pCO_2 from the sea surface made during a process study in the eastern equatorial Pacific Ocean are presented. During the study, a sampling device drew seawater from the upper few cm of the ocean into the laboratory of the research vessel for continuous measurements of pCO_2, pH, and DIC. A few intense rainstorms were encountered during the study, resulting in significant and systematic decreases in sea surface salinity, temperature, pCO_2, and DIC and increases in pH.

2. Methods

The measurements described here were made aboard the Research Vessel Roger Revelle (R/V Roger Revelle) as part of the Salinity Processes in the Upper Ocean Regional Study 2 (SPURS-2) (Lindstrom et al., 2019) from 16 October to 17 November 2017 (including transit to the study site). The ultimate goal of SPURS-2 was to understand the physical processes controlling the sources and sinks of freshwater in the ocean. The study took place in the eastern equatorial Pacific Ocean, centered at 10°N and 125°W over a 3-week period. The location at the intertropical convergence zone was selected to maximize the chance that freshwater pools resulting from convective rain events would be encountered during the research cruise.

The carbon chemistry study described here was an add-on project to take advantage of the detailed measurements of rain and thorough vertical characterization of the sea surface temperature and salinity during SPURS-2. During the cruise, underway measurements of carbonate system parameters (i.e., pCO_2, pH, and DIC) were made in seawater from two water intakes at different depths, the uncontaminated seawater intake of the ship located at ~5 m, and a specially designed sampling system (described in greater detail below) at ~2–3 cm below the sea surface.

2.1. Salinity Snake

To sample the near surface of the ocean, a specially designed system called the Salinity Snake was used during SPURS-2. The system consisted of two nylon-reinforced steel spiral rubber hoses (inner diameter: 2.54 cm) mounted on a boom (13.8 m long) on the starboard bow of the R/V Roger Revelle so that they are outside the wake of the ship. The hose is negatively buoyant but would follow the air-sea interface due to drag created at vessel speeds over 10 km hr^{-1} (~2.8 m s^{-1}). One hose was mounted at the end of the boom and used when the ship was moving faster than 10 km hr^{-1}, while the other, which has polychloroprene attached to the outside to increase buoyancy, was mounted 10-m outboard on the boom and used at speeds less than 10 km hr^{-1}. Temperature loggers (Sea-Bird SBE 56) were used to stopper the ends of the intake hoses and record the in situ sea surface temperature. Just upstream of the logger on each hose is a series of ten 6-mm water intake holes, spaced 3 cm apart.

An electrically actuated three-way T-valve (Valworx 563208E) was used to automatically switch between the two hoses at a threshold of 10 km hr^{-1}. Seawater is drawn through the hoses (total length ~60 m) with a peristaltic pump (Albin ALP-30; flow rate of 36–38 L min^{-1}) and delivered to the instruments in the lab. The residence time of water in the hose was 60–140 s. The flow rate was monitored and recorded by an electronic flow meter (Seametrics SPX-025).

2.2. pCO_2, pH, and DIC Measurements

During the cruise, automated continuous measurements of pCO_2, DIC, and pH were made on seawater pumped from the Salinity Snake using one set of instruments (called surface instruments here). In addition, another set of instruments (called 5-m instruments here) measured pCO_2 and pH on seawater pumped from the uncontaminated seawater intake of the ship, located at a nominal depth of 5 m.

Each source of water passed through a thermosalinograph (Sea-Bird SBE 45 MicroTSG) in the laboratory to enable determination of salinity and temperature before being sent to the analytical systems for the various carbonate system measurements. The temperatures of the seawater measured in the laboratory were

compared with temperature measured near the intake to correct for temperature changes (typically around −0.2°C to −0.3°C; i.e., water cools down in the laboratory due to air conditioning). The intake temperature for the 5-m seawater system was measured by a thermosalinograph (Sea-Bird SBE 45 MicroTSG) located in the bow thruster room of the R/V Roger Revelle, whereas temperature for the Salinity Snake was recorded at the tip of the hoses (as described above).

The design of the pCO_2 systems is described in detail in Ho, Wanninkhof, et al. (1997). Each system used a showerhead equilibrator coupled to a nondispersive infrared analyzer (NDIR analyzer; LI-COR LI-840A). They were calibrated with CO_2 free air generated by passing laboratory air through a column of soda lime and with two compressed CO_2 standards (nominal mixing ratios of 375 and 425 ppmv), referenced to a master CO_2 standard from NOAA/ESRL/GMD.

The DIC system, described in detail in Friederich et al. (2002), took a small volume (1.5 ml) of seawater, acidified it with phosphoric acid to convert all the HCO_3^- and CO_3^{2-} to CO_2, and sent the resulting gas to an NDIR analyzer (LI-COR LI-7000) for quantification by bubbling the mixture with CO_2 free gas. The system was calibrated using certified reference material for CO_2 (Dickson, 2010).

Seawater pH (total scale) from each source was measured inline using an ion sensitive field effect transistor-based pH sensor (Honeywell Durafet II). The sensor was chosen for its fast response (a few ms) and long-term stability (weeks) (Martz et al., 2010). The pH sensors were calibrated at the beginning, middle, and end of the cruise using certified reference material for CO_2 at sea surface temperatures, by determining the pH from DIC and TAlk using CO2SYS (van Heuven et al., 2011) and the dissociation constants of Lueker et al. (2000).

The pCO_2 and pH measurements on the Salinity Snake were made at a temporal resolution of 3 s, and the results were averaged to 1 min, and the pCO_2 and pH measurements on the 5-m seawater intake have a temporal resolution of ~1 min. The DIC system had a temporal resolution of ~3 min.

The surface instruments measured pCO_2, DIC, and pH from the surface water whenever the Salinity Snake was deployed. At other times, the surface instruments were used to measure seawater from the 5-m seawater intake of the R/V Roger Revelle to compare results with the 5-m instruments that were making simultaneous measurements of pCO_2 and pH from the same water stream.

A total of 592,452, 9,883, and 650,418 measurements of pCO_2, DIC, and pH, respectively, was made from the Salinity Snake using the surface instruments, and a total of 30,937 and 17,529 measurements of pCO_2 and pH, respectively, was made from the uncontaminated seawater intake using the 5-m instruments.

3. Results and Discussion

During SPURS-2, 8 large freshwater pools, referred to here as "puddles" and defined as times when salinity measured between the Salinity Snake and the 5-m intake of the ship differed by more than 0.5 over a few km, were encountered. Since the starting DIC and TAlk were similar for all the puddles, the resulting changes in pCO_2 due to rain were likewise similar. In the interest of conserving space and having a more focused discussion, the analysis here will evaluate two of the larger puddles, one from YD 298 (25 October 2017) and another from YD 313 (9 November 2017). It is difficult to ascertain the horizontal dimensions of these puddles since the ship only traversed them in one direction, and it is not clear which part of the puddle was being sampled. Nevertheless, the largest of two puddles examined here was at least ~52 km wide and was characterized by a decrease in sea surface salinity of up to 4.4, a decrease in sea surface temperature of 1.3°C, and a pCO_2 decrease of 84 μatm (Figure 1).

3.1. Measured Versus Calculated pCO_2

A major difference between the pCO_2 measurements made by the surface instruments compared to the DIC and pH measurements is how representative they are of the values at a given location and time. The DIC and pH measurements were essentially instantaneous because the pH sensor was in the water stream and the DIC system isolated a small volume of water for measurement. However, pCO_2 was measured in the headspace gas of an equilibrator that was continuously equilibrated with flowing seawater (flow rate ~1.5 to 2 L min^{-1}), and this headspace was circulated through the NDIR analyzer at ~200–300 ml min^{-1}. The analysis system for pCO_2 acted as a low-pass filter with a phase lag, because of the time it takes for CO_2 in the

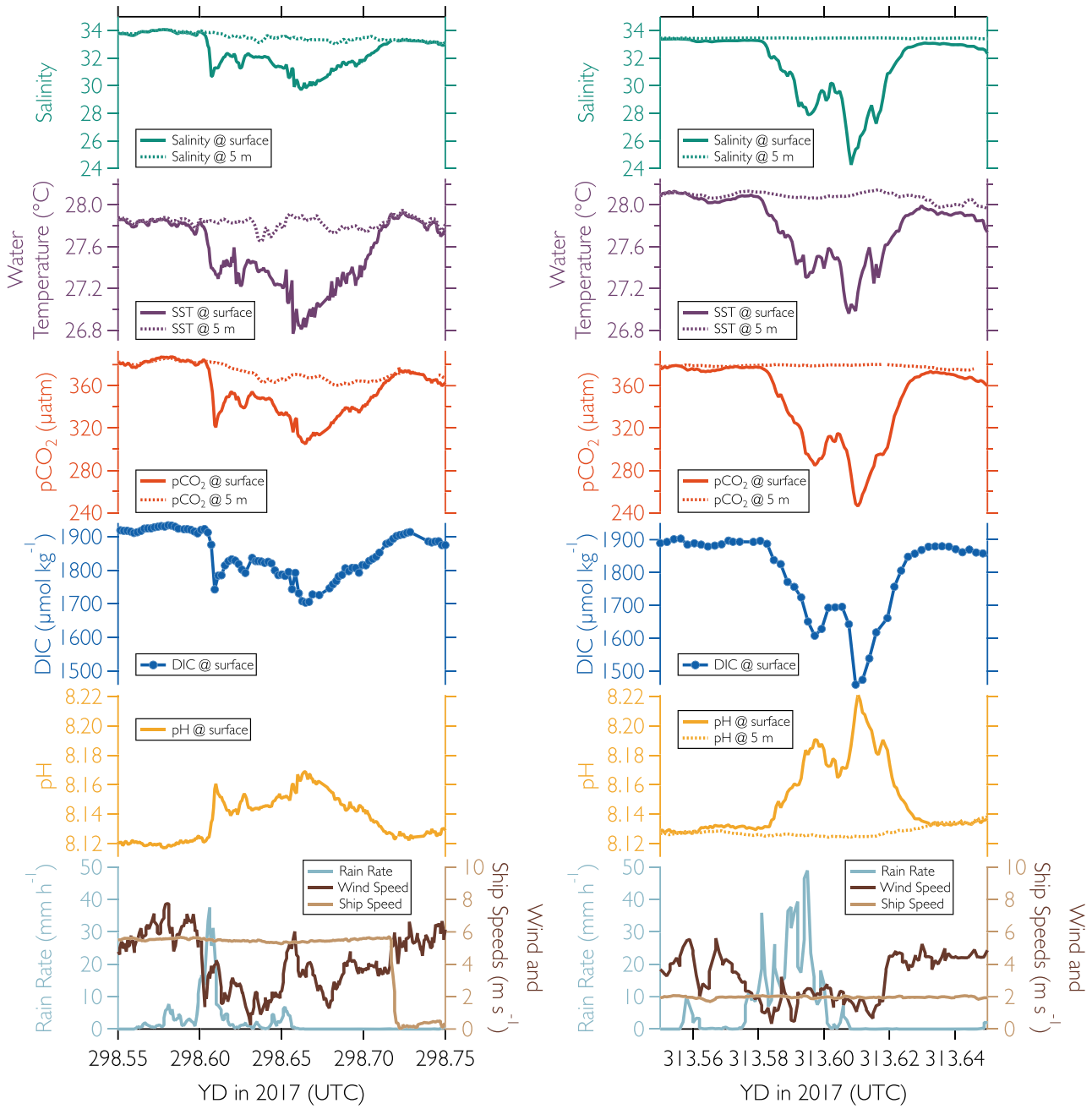

Figure 1. Time series of salinity, water temperature, pCO_2, DIC, pH, rain rate, wind speed, and ship speed for two of the puddles encountered during SPURS-2. Waterside parameters from the Salinity Snake and from the 5-m intake of the ship are shown where available. All parameters were measured, except pCO_2 from the Salinity Snake, which was calculated from measured DIC and pH. No pH measurements were available from the 5-m water intake on YD 298.

water to equilibrate with gas in the headspace, the time required to flush the water in the equilibrator, and the time required for the gas to circulate through the relatively large headspace (~1 L), the tubing, and NDIR analyzer cell. The resulting pCO_2 measurements resemble an ~15-min running average of the pCO_2 in the water (see supporting information). Hence, the system was suited for measuring underway pCO_2 during most conditions but would underestimate the deviation from the mean when the pCO_2 changed rapidly, such as when the ship transected a puddle.

Measured values of DIC and pH were used to calculate pCO_2 using CO2SYS and the dissociation constants of Lueker et al. (2000) for comparison. During normal (i.e., nonrain) conditions, these calculated pCO_2 values

are in close agreement with the measured pCO_2 values (root-mean-square error [RMSE]: 1.5 to 2.5 μatm). However, during and after rain events, significant differences exist (RMSE: 5 to 17 μatm). To obtain instantaneous values of pCO_2, the calculated values are used here in the analysis (see supporting information for comparison between measured and calculated pCO_2). Extensive comparisons were made between the measured and calculated pCO_2 values outside of the puddles to ensure that they agree within the expected RMSE (~2 μatm).

3.2. Measurements at the Surface Versus 5 m

Comparing the measurements made by the surface and 5-m instruments, it is clear that rain can significantly dilute the sea surface salinity relative to 5-m depth, and the dilution also affects the carbonate system parameters. Figure 1 shows that during both YD 298 and 313, when the ship encountered the puddles, the surface salinity dropped rapidly, and this drop was accompanied by rapid changes in surface pCO_2, DIC, and pH relative to measurements at 5-m depth.

Also shown in the figures is the rain rate, indicating that the rain had largely stopped during the transect of the YD 298 puddle, whereas it was still raining fairly heavily during the early part of the YD 313 puddle. This difference in rain conditions gives an indication of how long the surface anomaly has had to mixed down to 5 m. On YD 298, the changes in salinity and pCO_2 (as well as the other parameters) are seen even from the instrument at 5 m, although the magnitude of the changes is not as great.

3.3. Effect of Dilution and Temperature Change on pCO_2

Besides adding freshwater to the sea surface and lowering salinity, rain is often colder than the seawater, causing a decrease in sea surface temperature. Both of these effects can change sea surface pCO_2. For example, for the puddles from YD 298 and 313, the maximum salinity changes were 4.4 and 9.3, respectively, and the change in sea surface temperatures was 1.3°C for both puddles. The observed decreases in pCO_2 were 84 and 135 μatm for YD 298 and 313, respectively, and nearly 88% and 93% of the decrease for YD 298 and 313, respectively, were due to salinity dilution, with the rest due to temperature changes.

3.4. Relationship Between Salinity and DIC, pCO_2, and pH

The concentration of DIC decreased linearly as a function of salinity because rainfall on the sea surface dilutes DIC concentration in a straightforward manner. Rainwater contains a small amount of DIC in the form of dissolved CO_2. This DIC concentration is proportional to atmospheric pCO_2 and modulated by air temperature, which determines the amount of CO_2 that will dissolve in the raindrops. The DIC concentration in surface seawater at any given time during and after a rain dilution event, $[DIC_t]$, could be predicted using the measured salinity as follows:

$$[DIC_t] = [DIC_i]\left(\frac{S_t}{S_i}\right) + [DIC_r]\left(1 - \frac{S_t}{S_i}\right), \tag{2}$$

where $[DIC_i]$ is the initial DIC concentration (i.e., before any rain-induced perturbation), $[DIC_r]$ is the concentration of DIC in the raindrops, S_i is the initial sea surface salinity, and S_t is the measured sea surface salinity at time t. During SPURS-2, the atmospheric CO_2 was 405.1 ppm (Peters et al., 2007), and given an average measured air temperature of 25.5–26°C and relative humidity of 80% to 90%, the dew point was ~23°C, and the amount of DIC in the raindrops is calculated to be 14.6 μmol kg^{-1} using the solubility relationship of Weiss (1974).

Similarly, even though TAlk was not measured during SPURS-2, it could be calculated from pCO_2 and DIC using CO2SYS (van Heuven et al., 2011). TAlk at any given time t, $[TAlk_t]$, could be predicted as follows:

$$[TAlk_t] = [TAlk_i]\left(\frac{S_t}{S_i}\right), \tag{3}$$

where $[TAlk_i]$ is the initial TAlk concentration, and rain is assumed to contribute no alkalinity.

Unfortunately, there is no single equation to describe the relationship between salinity and pCO_2 or pH, since the changes in pCO_2 and pH as a function of dilution depend on the initial DIC and TAlk

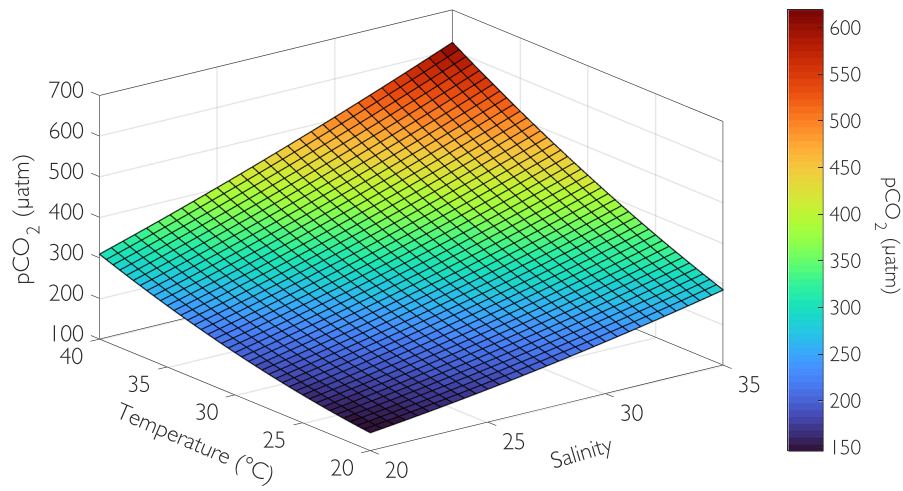

Figure 2. Modeled pCO_2 as a function of sea surface temperature and salinity determined at DIC and TAlk concentrations of 1,900 and 2,211 μmol kg^{-1}, respectively, and at a starting temperature of 40°C and salinity of 35.

concentrations, as well as the seawater temperature. Furthermore, the relationship between pCO_2 (or pH) and salinity is nonlinear, because of the nonlinearity between pCO_2 (or pH) and DIC as well as TAlk.

At a fixed starting DIC and TAlk, it is possible to predict the change in pCO_2 as a function of temperature and salinity. For example, assuming environmental conditions similar to what was experienced during SPURS-2 (i.e., DIC of 1,900 and TAlk of 2,211, at a starting salinity of 35) and using CO2SYS (van Heuven et al., 2011) and the dilution of DIC and TAlk is as described by Equations 2 and 3, pCO_2 as a function of temperature (T) and salinity (S) can be predicted using the following equation (Figure 2):

$$pCO_2 = 339.2547 - 12.9564\,S - 16.3947\,T + 0.1999\;S^2 + 0.5639\,S\,T + 0.2217\,T^2. \tag{4}$$

As can be seen in Figure 2, even though the percent decrease in pCO_2 due to salinity dilution from 35 to 20 is similar in the range of temperatures from 20°C to 40°C, because the pCO_2 is higher at the warmer temperatures (by ~2× between 20°C and 40°C), the change in pCO_2 is also substantially greater (by ~2×).

For SPURS-2, the relationships between pCO_2 and salinity and between pH and salinity are shown in Figure 3. The pCO_2 data in Figure 3 have been calculated at the 5-m temperature, and therefore represent primarily the influence of dilution. Also shown in Figure 3 are the pCO_2 and DIC changes predicted by Equations 2 and 4, and overall, they are able to predict the observed pCO_2 and DIC to a reasonable degree (RMSE for pCO_2: 7.5 μatm; RMSE for DIC: 7.4 μmol kg^{-1}).

3.5. Implications for Global CO_2 Fluxes

Determining CO_2 fluxes from pCO_2 disequilibrium requires knowing both the k_{CO_2} and Δp_{CO_2}. Since global maps of surface ocean pCO_2, such as those from Landschützer et al. (2016), Rödenbeck et al. (2015), or Takahashi et al. (2009), are constructed from ship-based measurements made at 5 m, the CO_2 fluxes calculated using these global pCO_2 maps might underestimate the actual ocean CO_2 uptake depending on the prevalence, magnitude, and duration of the pCO_2 anomalies described here. Even if the increase in global CO_2 uptake is small (e.g., 5%), it could still represent a nonnegligible portion of the missing CO_2 sink of 1.6 $GtCO_2\,yr^{-1}$ for the last decade (Friedlingstein et al., 2019). Furthermore, rain on the ocean could increase CO_2 uptake by increasing k_{CO_2} (Ho et al., 2004; Zappa et al., 2009), especially when wind speeds are low (Harrison et al., 2012).

The two published modeling studies that have examined the effect of rainfall on air-sea CO_2 fluxes (Ashton et al., 2016; Turk et al., 2010) have made simplified assumptions about either the salinity stratification of the sea surface or have ignored changes in surface ocean salinity and pCO_2 altogether, which make those studies unsuitable for determining the global effects of rain on air-sea CO_2 fluxes.

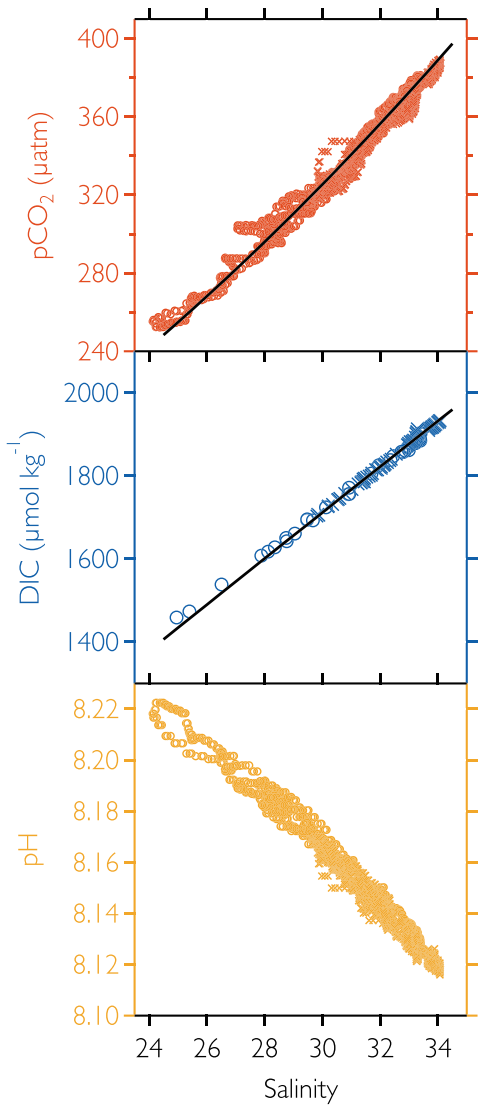

Figure 3. pCO_2, DIC, and pH plotted against sea surface salinity for the periods displayed in Figure 1. DIC and pH were measured; pCO_2 was calculated from DIC and pH using the 5-m temperature and so does not include the changes due to rain-induced cooling of the sea surface. The crosses and open circles are data for YD 298 and 313, respectively. Also shown as black lines are pCO_2 and DIC predicted by Equations 4 and 2, respectively.

The modeling study by Turk et al. (2010) focused on one year at one location in the western equatorial Pacific and showed that rain-induced changes in sea surface pCO_2 could turn a CO_2 source region into a sink region. However, in that study, the details of the rain-induced salinity stratification were largely ignored, and the relaxation back to initial conditions was assumed to be independent of oceanic and meteorological conditions. The stratified layer depth and time scale for dissipation of the rain signal were assumed to be the same as the mixed layer and mixing time scale observed in the Biosphere 2 ocean during a series of rain experiment there (Zappa et al., 2009). The Biosphere 2 ocean is about the size of a large swimming pool (surface area of 35 × 20 m), with a maximum depth of 6 m. It is equipped with a vacuum wave generator on one end and a beach on the other. Because of the lack of wind inside Biosphere 2, mechanical pumps in the ocean were used to bring water from depth up to the surface, leading to distinctly different mixing characteristics than the open ocean.

In the other study, Ashton et al. (2016) examined the effect of rain on air-sea CO_2 fluxes and concluded that there could be significant differences in air-sea CO_2 fluxes between rain and no rain conditions, but the phenomena of changes in SSS and its effect on surface ocean pCO_2 were explicitly ignored. Hence, the effect of rain on CO_2 fluxes on regional and global scales is still uncertain.

3.6. The Way Forward

At present, there are no global determinations of what the typical magnitude of the salinity and pCO_2 anomalies from rain events are, how long the dilution events last, and how widespread they are. Studies have shown that rain-induced changes in sea surface salinity are a function of rain intensity, and the duration of the salinity anomalies depends mainly on wind speeds (e.g., Asher et al., 2014; Bellenger et al., 2017; Drushka et al., 2016). These salinity anomalies typically last only a few hours (Reverdin et al., 2020), but at low wind speeds, they could last longer than 20 hr (e.g., Boutin et al., 2014; Price, 1979; Thompson et al., 2019).

The next step is to examine how this surface dilution in salinity and pCO_2 translates to changes in global CO_2 fluxes. One way to do this is to use an existing model for predicting sea surface salinity as a function of rain rate, wind speed, and radiative forcing (e.g., Bellenger et al., 2017) and determine the duration and magnitude of global sea surface salinity anomalies. That information can then be used to modify global maps of sea surface pCO_2 and determine the resulting CO_2 fluxes. Since the relationship between pCO_2 and salinity is nonlinear and dependent on DIC and TAlk concentrations, global maps of TAlk (e.g., Broullón et al., 2019) and of DIC can be used to propagate the dilution signal, where the maps of DIC are constructed from maps of sea surface pCO_2 (e.g., Landschützer et al., 2016) and TAlk.

Efforts should also be made to make sea surface pCO_2 measurements closer to the surface. Some autonomous vehicles (e.g., Wave Gliders and Saildrones) are currently measuring pCO_2 in the surface ocean at depths shallower than 5 m, and these sampling methods should increase, especially in areas of the ocean that are difficult to sample (e.g., the Southern Ocean in winter). Also, in certain global class research vessels in the UNOLS fleet (e.g., R/V Roger Revelle and R/V Thomas G. Thompson), seawater sampling ports have been installed at 2 and 3 m, and water from these ports could be used for measurements of pCO_2, pH, and DIC. Due to hydrodynamics of water flow around the bow of the research vessel, the water sampled at these 2- and 3-m ports are in fact from a shallower depth (i.e., the water gets pushed down to those depths) which would give a better representation of sea surface pCO_2, whereas the 5-m port actually samples water from ~5 m.

4. Conclusions

The measurements from the eastern tropical Pacific show that because sea surface pCO_2 is usually measured at 5-m depth, the pCO_2 close to the sea surface is missed, which is relevant for determining Δp_{CO_2} and air-sea CO_2 fluxes. This is important when pCO_2 near the surface differs significantly from that at 5 m, such as during and after rain events. This difference has important implications for using the pCO_2 disequilibrium method to determine air-sea CO_2 fluxes because, with rainfall, the absolute magnitude of the Δp_{CO_2} is decreased in source regions and increased in sink regions, leading to decrease in CO_2 outgassing in source regions and increase in CO_2 uptake in sink regions, with a net increase of CO_2 by the ocean. Efforts should be made to determine the global significance of this effect and to make measurements closer to the surface.

Data Availability Statement

The meteorological and surface ocean data used in the analysis here could be downloaded from NASA PO.DAAC (https://doi.org/10.5067/SPUR2-USPS0; https://doi.org/10.5067/SPUR2-MET00). The carbonate chemistry data could be downloaded from NASA PO.DAAC (https://doi.org/10.5067/SPUR2-PCO20) and are also included in supporting information.

Acknowledgments
We thank G. Friederich and B. Hickman for assistance with instrument setup and data reduction, the crew of the R/V Roger Revelle for assistance during the cruise, W. Asher for helpful discussions during and after the cruise, and R. Wanninkhof and an anonymous reviewer for suggestions that improved the manuscript. Funding was provided by National Aeronautics and Space Administration Physical Oceanography Program (NNX15AF73G and 80NSSC18K1496).

References

Asher, W. E., Jessup, A. T., Branch, R., & Clark, D. (2014). Observations of rain-induced near-surface salinity anomalies. *Journal of Geophysical Research: Oceans*, *119*, 5483–5500. https://doi.org/10.1002/2014JC009954

Ashton, I. G., Shutler, J. D., Land, P. E., Woolf, D. K., & Quartly, G. D. (2016). A sensitivity analysis of the impact of rain on regional and global sea-air fluxes of CO_2. *PLoS ONE*, *11*, e0161105. https://doi.org/10.1371/journal.pone.0161105

Bellenger, H., Drushka, K., Asher, W., Reverdin, G., Katsumata, M., & Watanabe, M. (2017). Extension of the prognostic model of sea surface temperature to rain-induced cool and fresh lenses. *Journal of Geophysical Research: Oceans*, *122*, 484–507. https://doi.org/10.1002/2016JC012429

Boutin, J., Martin, N., Reverdin, G., Morisset, S., Yin, X., Centurioni, L., & Reul, N. (2014). Sea surface salinity under rain cells: SMOS satellite and in situ drifters observations. *Journal of Geophysical Research: Oceans*, *119*, 5533–5545. https://doi.org/10.1002/2014JC010070

Broullón, D., Pérez, F. F., Velo, A., Hoppema, M., Olsen, A., Takahashi, T., et al. (2019). A global monthly climatology of total alkalinity: A neural network approach. *Earth System Science Data*, *11*(3), 1109–1127. https://doi.org/10.5194/essd-11-1109-2019

Dickson, A. G. (2010). Standards for ocean measurements. *Oceanography*, *23*(3), 34–47. https://doi.org/10.5670/oceanog.2010.22

Dlugokencky, E. J., J. W. Mund, A. M. Crotwell, M. J. Crotwell, & K. W. Thoning (2019). Atmospheric carbon dioxide dry air mole fractions from the NOAA ESRL carbon cycle cooperative global air sampling network, 1968-2018, Version: 2019–2007, https://doi.org/10.15138/wkgj-f215

Drushka, K., Asher, W. E., Ward, B., & Walesby, K. (2016). Understanding the formation and evolution of rain-formed fresh lenses at the ocean surface. *Journal of Geophysical Research: Oceans*, *121*, 2673–2689. https://doi.org/10.1002/2015JC011527

Friederich, G. E., Walz, P. M., Burczynski, M. G., & Chavez, F. P. (2002). Inorganic carbon in the Central California upwelling system during the 1997–1999 El Niño–La Niña event. *Progress in Oceanography*, *54*(1-4), 185–203. https://doi.org/10.1016/S0079-6611(02)00049-6

Friedlingstein, P., Jones, M. W., O'Sullivan, M., Andrew, R. M., Hauck, J., Peters, G. P., et al. (2019). Global carbon budget 2019. *Earth System Science Data*, *11*(4), 1783–1838. https://doi.org/10.5194/essd-11-1783-2019

Harrison, E. L., Veron, F., Ho, D. T., Reid, M. C., Orton, P., & McGillis, W. R. (2012). Nonlinear interaction between rain and wind induced air-water gas exchange. *Journal of Geophysical Research*, *117*, C03034. https://doi.org/10.1029/2011JC007693

Ho, D. T., Bliven, L. F., Wanninkhof, R., & Schlosser, P. (1997). The effect of rain on air-water gas exchange. *Tellus*, *49*(2), 149–158. https://doi.org/10.1034/J.1600-0889.49.Issue2.3.X

Ho, D. T., Law, C. S., Smith, M. J., Schlosser, P., Harvey, M., & Hill, P. (2006). Measurements of air-sea gas exchange at high wind speeds in the Southern Ocean: Implications for global parameterizations. *Geophysical Research Letters*, *33*, L16611. https://doi.org/10.1029/2006GL026817

Ho, D. T., Wanninkhof, R., Masters, J., Feely, R. A., & Cosca, C. E. (1997). Measurement of underway fCO_2 in the eastern equatorial Pacific on NOAA ships MALCOLM BALDRIGE and DISCOVERER from February to September, 1994. *Rep ERL AOML-30*, 52 pp, NTIS Springfield.

Ho, D. T., Zappa, C. J., McGillis, W. R., Bliven, L. F., Ward, B., Dacey, J. W. H., et al. (2004). Influence of rain on air-sea gas exchange: Lessons from a model ocean. *Journal of Geophysical Research*, *109*, C08S18. https://doi.org/10.1029/2003JC001806

Landschützer, P., Gruber, N., & Bakker, D. C. E. (2016). Decadal variations and trends of the global ocean carbon sink. *Global Biogeochemical Cycles*, *30*, 1396–1417. https://doi.org/10.1002/2015GB005359

Lindstrom, E. J., Edson, J. B., Schanze, J. J., & Shcherbina, A. Y. (2019). SPURS-2: Salinity Processes in the Upper-Ocean Regional Study 2—The eastern equatorial Pacific experiment. *Oceanography*, *32*(2), 15–19. https://doi.org/10.5670/oceanog.2019.207

Lueker, T. J., Dickson, A. G., & Keeling, C. D. (2000). Ocean pCO_2 calculated from dissolved inorganic carbon, alkalinity, and equations for K1 and K2: Validation based on laboratory measurements of CO_2 in gas and seawater at equilibrium. *Marine Chemistry*, *70*(1-3), 105–119. https://doi.org/10.1016/S0304-4203(00)00022-0

Martz, T. R., Connery, J. G., & Johnson, K. S. (2010). Testing the Honeywell Durafet® for seawater pH applications. *Limnology and Oceanography: Methods*, *8*(5), 172–184. https://doi.org/10.4319/Lom.2010.8.172

Masarie, K. A., & Tans, P. P. (1995). Extension and integration of atmospheric carbon dioxide data into a globally consistent measurement record. *Journal of Geophysical Research*, *100*(D6), 11,593–11,610. https://doi.org/10.1029/95JD00859

McNeil, C. L., & Merlivat, L. (1996). The warm oceanic surface layer: Implications for CO_2 fluxes and surface gas measurements. *Geophysical Research Letters*, *23*(24), 3575–3578. https://doi.org/10.1029/96GL03426

Nightingale, P. D., Malin, G., Law, C. S., Watson, A. J., Liss, P. S., Liddicoat, M. I., et al. (2000). In situ evaluation of air-sea gas exchange parameterizations using novel conservative and volatile tracers. *Global Biogeochemical Cycles*, *14*(1), 373–387. https://doi.org/10.1029/1999GB900091

Peters, W., Jacobson, A. R., Sweeney, C., Andrews, A. E., Conway, T. J., Masarie, K., et al. (2007). An atmospheric perspective on North American carbon dioxide exchange: CarbonTracker. *Proceedings of the National Academy of Sciences*, *104*(48), 18,925–18,930. https://doi.org/10.1073/pnas.0708986104

Price, J. F. (1979). Observations of a rain-formed mixed layer. *Journal of Physical Oceanography*, *9*(3), 643–649. https://doi.org/10.1175/1520-0485(1979)009<0643:Ooarfm>2.0.Co;2

Reverdin, G., Supply, A., Drushka, K., Thompson, E. J., Asher, W. E., & Lourenço, A. (2020). Intense and small freshwater pools from rainfall investigated suring SPURS-2 on 9 November 2017 in the eastern tropical Pacific. *Journal of Geophysical Research: Oceans*, *125*, e2019JC015558. https://doi.org/10.1029/2019JC015558

Robertson, J. E., & Watson, A. J. (1992). Thermal skin effect of the surface ocean and its implications for CO_2 uptake. *Nature*, *358*(6389), 738–740. https://doi.org/10.1038/358738a0

Rödenbeck, C., Bakker, D. C. E., Gruber, N., Iida, Y., Jacobson, A. R., Jones, S., et al. (2015). Data-based estimates of the ocean carbon sink variability—First results of the surface ocean CO_2 mapping intercomparison (SOCOM). *Biogeosciences*, *12*, 7251–7278. https://doi.org/10.5194/bg-12-7251-2015

Takagaki, N., & Komori, S. (2007). Effects of rainfall on mass transfer across the air-water interface. *Journal of Geophysical Research*, *112*, C06006. https://doi.org/10.1029/2006JC003752

Takahashi, T., Sutherland, S. C., Wanninkhof, R., Sweeney, C., Feely, R. A., Chipman, D. W., et al. (2009). Climatological mean and decadal change in surface ocean pCO_2, and net sea-air CO_2 flux over the global oceans. *Deep-Sea Research Part II*, *56*(8–10), 554–577. https://doi.org/10.1016/j.dsr2.2008.12.009

Thompson, E. J., Moum, J. N., Fairall, C. W., & Rutledge, S. A. (2019). Wind limits on rain layers and diurnal warm layers. *Journal of Geophysical Research: Oceans*, *124*, 897–924. https://doi.org/10.1029/2018JC014130

Turk, D., Zappa, C. J., Meinen, C. S., Christian, J. R., Ho, D. T., Dickson, A. G., & McGillis, W. R. (2010). Rain impacts on CO_2 exchange in the western equatorial Pacific Ocean. *Geophysical Research Letters*, *37*, L23610. https://doi.org/10.1029/2010GL045520

van Heuven, S., Pierrot, D., Rae, J. W. B., Lewis, E., & Wallace, D. W. R. (2011). MATLAB program developed for CO_2 system calculations, *Rep*, ORNL/CDIAC-105b, Carbon Dioxide Inf. Anal. Cent., Oak Ridge Natl. Lab., US DOE, Oak Ridge, Tennis

Van Scoy, K. A., Morris, K. P., Robertson, J. E., & Watson, A. J. (1995). Thermal skin effect and the air-sea flux of carbon dioxide: A seasonal high-resolution estimate. *Global Biogeochemical Cycles*, *9*(2), 253–262. https://doi.org/10.1029/94GB03356

Wanninkhof, R., Asher, W. E., Ho, D. T., Sweeney, C., & McGillis, W. R. (2009). Advances in quantifying air-sea gas exchange and environmental forcing. *Annual Review of Marine Science*, *1*(1), 213–244. https://doi.org/10.1146/annurev.marine.010908.163742

Weiss, R. F. (1974). Carbon dioxide in water and seawater: The solubility of a non-ideal gas. *Marine Chemistry*, *2*(3), 203–215. https://doi.org/10.1016/0304-4203(74)90015-2

Woolf, D. K., Land, P. E., Shutler, J. D., Goddijn-Murphy, L. M., & Donlon, C. J. (2016). On the calculation of air-sea fluxes of CO_2 in the presence of temperature and salinity gradients. *Journal of Geophysical Research: Oceans*, *121*, 1229–1248. https://doi.org/10.1002/2015JC011427

Woolf, D. K., Shutler, J. D., Goddijn-Murphy, L., Watson, A. J., Chapron, B., Nightingale, P. D., et al. (2019). Key uncertainties in the recent air-sea flux of CO_2. *Global Biogeochemical Cycles*, *33*, 1548–1563. https://doi.org/10.1029/2018GB006041

Zappa, C. J., Ho, D. T., McGillis, W. R., Banner, M. L., Dacey, J. W. H., Bliven, L. F., et al. (2009). Rain-induced turbulence and air-sea gas transfer. *Journal of Geophysical Research*, *114*, C07009. https://doi.org/10.1029/2008JC005008